

Significance of Mixing Matrix Structure on Principal Component-Based Analysis of Atrial Fibrillation Body Surface Potential Maps

P Bonizzi¹, MS Guillem², F Castells², AM Climent², V Zarzoso¹, O Meste¹

¹Laboratoire I3S UNSA - CNRS, Sophia Antipolis, France

²ITACA - Bioingeniera, Universitat Politecnica de Valencia, España

Abstract

Atrial fibrillation (AF) type classifiers are still hardly accepted in clinical practice due to their invasive approach. In this work a new automated method to assess noninvasively different AF types is presented, based on the high spatial resolution given by body surface potential maps (BSPM). AF organization degree was assessed by its influence on the spatio-temporal pseudostationarity and complexity of a principal component analysis mixing matrix repeatedly derived along a BSPM recording. Stationarity was analyzed in terms of ability of the mixing matrix derived for a specific recording segment to retrieve the AA components of subsequent segments, while complexity in terms of its number of significant components. Results show that AF organization is reflected in a greater pseudostationarity of the mixing matrix along the recordings and in a lower number of components needed to represent the AA, interpreted as a lower complexity in the underlying AA in patients with organized AF type I.

1. Introduction

Despite of the observation that during atrial fibrillation (AF) the atrial tissue is activated by multiple wavelets showing uncoordinated patterns, several studies have demonstrated the presence of organization of atrial activation processes, indicating that a certain degree of local organization exists during AF, likely caused by deterministic mechanisms of activation [1], and inversely depending on the chronification of the pathology [2].

Previous invasive studies have attempted to distinguish between organized and disorganized electrical activity during AF. Exploiting principal component analysis (PCA), Faes *et al.* [3] noted that electrograms recorded at different sites presenting different atrial activity (AA) organization were characterized by a different number of significant principal components, with a lower number of components needed to represent the more organized AA. Nonetheless, invasive AF classification is still hardly accepted in clinical

practice despite its potential relevance in clinical decision making. Therefore, assessment and classification of AF types from a noninvasive procedure would be appreciated. Guillem *et al.* [4] demonstrated the possibility of a non-invasive visual evaluation of different activation patterns in patient with AF, similar to that observed invasively by Konings *et al.* [5], but exploiting the high spatial resolution given by body surface potential maps (BSPM), a technique which has the advantage over the conventional ECG of a much higher spatial resolution.

In line with these findings, and exploiting the attested ability of PCA to be a valuable tool for addressing diverse issues in ECG analysis [6], this work aims to test the possibility of an automated noninvasive evaluation of different AF types, analyzing if the degree of AF spatio-temporal repetitiveness and organization can be noninvasively assessed through its influence on the spatio-temporal pseudostationarity and complexity of a PCA mixing matrix repeatedly derived along a BSPM recording.

2. Methods

2.1. BSPM data and acquisition system

A dataset composed of 10 BSPM recordings was employed. All recordings presented persistent AF, 5 previously classified as AF type I (single wavefront propagating across the body surface) and 5 as AF type III (no observable clear wavefront or multiple wavefronts that do not propagate across the body surface observed simultaneously), according to the same criteria and terminology for classification as those of Konings *et al.* [5], although applied to surface recordings instead of electrograms. The acquisition system exploited was the same as the one introduced in [4]. By means of it, a total of 56 chest and back leads were acquired simultaneously for each subject. Leads were arranged as shown in Fig. 1(a). All recordings were 1-minute long. In order to point out possible differences in the spatial stationarity and organization of the wavefront patterns between the two AF types, no AF signals classified as type II have been considered in this study.

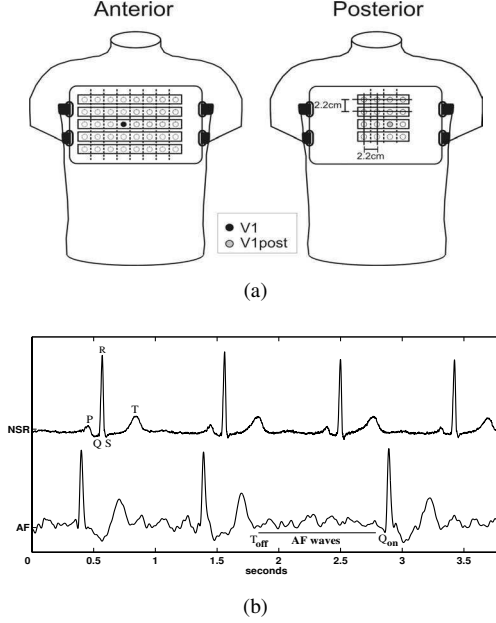


Figure 1. (a) Arrangement of the electrodes (open circles) and belt used for their attachment to the patient. (b) Definition of the different cardiac waves and intervals. At the top, example of normal sinus rhythm ECG (NSR). At the bottom, example of AF ECG, showing a TQ interval (off:offset; on:onset).

AF type I and III recordings have been always analyzed as two separated groups in this study.

2.2. ECG signal preprocessing

ECG signals were processed by applying a third-order zerophase high-pass Chebyshev filter with a -3 dB cut off frequency at 0.5 Hz to remove baseline wandering due to physiologically irrelevant low frequency signal interferences (<1 Hz) [7], followed by a third-order zerophase low-pass Chebyshev filter with a -3 dB cut off frequency at 100 Hz to remove high frequency noise. Finally, a zerophase notch filter at 50 Hz was used to suppress power line noise.

2.3. Atrial activity recordings

In this study only ECG segments free from ventricular activity were analyzed, and the AA hidden by the QRS-T complex was disregarded. For this purpose, the R wave peak, the Q wave onset, and the T wave offset were detected (see Fig. 1(b) for the delineation of the different cardiac waves). Each BSPM recording was split in 6 consecutive intervals of 10-s, and an AA signal was derived for each interval concatenating only the TQ segments inside it. In this way, 6 consecutive 56 lead AA recordings

(named y_s , with $s = 1, \dots, 6$) were obtained from each 56 lead BSPM signal.

2.4. Principal component analysis

Spatial decorrelation provided by PCA involves a linear transformation of the mean corrected observed signals $\mathbf{y} \in \mathbb{R}^n$, which produces a set of uncorrelated waveforms with unit variance $\hat{\mathbf{x}} \in \mathbb{R}^m$ with ($m \leq n$)

$$\mathbf{y} = \mathbf{M}\mathbf{x} \Rightarrow \hat{\mathbf{x}} = \mathbf{M}^\# \mathbf{y} \quad (1)$$

where $\hat{\mathbf{x}}$ is an estimate of the true vector of the unknown components, \mathbf{M} is the mixing matrix, and symbol $\#$ stands for the pseudo-inverse operator. PCA reduces the dataset of observed signals to a few representative components, which are in decreasing order of variance accounted for in the observations. The ability of PCA to concentrate the original information in only k components can be assessed by the cumulative normalized variance, an index reflecting how well the subset of the first k principal components approximates the ensemble of original observations in energy terms

$$v_k = \frac{\sum_{i=1}^k \sigma_i^2}{\sum_{i=1}^m \sigma_i^2} \quad (2)$$

where σ_i are the singular values of \mathbf{y} .

2.5. AA spatio-temporal repetitiveness

In order to investigate the link between the complexity of the AF organization and the spatio-temporal repetitiveness in the propagation of its wavefront patterns, we analyzed the ability of the PCA mixing matrix derived for the first AA recording \mathbf{y}_1 to retrieve the AA components of subsequent segments. Similarly to what proposed by Rieta *et al.* in [8], we applied \mathbf{M}_1 to the following 5 AA recordings. In mathematical terms, given the PCA model (1) for \mathbf{y}_1 the associated mixing matrix \mathbf{M}_1 is retained and used to derive an estimate of the unknown components of the following AA recordings

$$\hat{\mathbf{x}}_s = \mathbf{M}_1^\# \mathbf{y}_s \quad \text{with } s = 2, \dots, 6 \quad (3)$$

where $\hat{\mathbf{x}}_s$ is the estimate of the component vector associated to segment s , obtained by \mathbf{M}_1 . Then, only the first k components of $\hat{\mathbf{x}}_s$ were selected to be reprojected back so as to reconstruct an estimate for \mathbf{y}_s

$$\hat{\mathbf{y}}_s = \sum_{i=1}^k \mathbf{m}_1^i \hat{x}_s^i \quad (4)$$

where \mathbf{m}_1^i is the i -th column of \mathbf{M}_1 , and \hat{x}_s^i the i -th component of $\hat{\mathbf{x}}_s$. A specific k giving v_k higher than 0.95 ($k_{0.95}$) was calculated for \mathbf{y}_1 of each subject, and used for deriving

all other \hat{y}_s in the same subject. Mixing matrix pseudostationarity was evaluated in terms of similarities between the original observations \mathbf{y}_s and the reconstructed ones $\hat{\mathbf{y}}_s$, by means of Pearson's coefficient (ρ) and normalized mean squared error (NMSE), on lead V1 only (lead containing most of the information on AA). NMSE was defined as

$$\text{NMSE} = \frac{\sum_{i=1}^N (y(i) - \hat{y}(i))^2}{\sum_{i=1}^N y(i)^2} \quad (5)$$

where $y(i)$ denotes the reference signal, $\hat{y}(i)$ an estimate of it, and N its length.

2.6. AA organization

In order to investigate the link between the complexity of the AF organization and the complexity in the propagation of the different wavefront patterns, we assumed that a less complex organization should be reflected in a lower number of significant components needed to represent the AA. Hence, we looked at the average value of parameters $k_{0.95}$ derived over all PCA mixing matrices \mathbf{M}_s on the same patient. Indeed, when the eigenvalues associated to the first components are much larger than those associated to other components, the ensemble exhibits a low morphological variability, whereas a slow fall-off of the principal components values indicates a large variability, and so a higher complexity of the underlying AA.

2.7. Combined analysis

Pseudostationarity analysis described in Section 2.5 was performed again keeping fixed the number of components k for the reconstruction of any \hat{y}_s , in all subjects. The number of components k was fixed at the mean value $\bar{k}_{0.95}^{AFI}$ obtained analyzing AF type I recordings only. In that way, we wanted to test the improbability of having a highly disorganized AA which somehow presents a spatio-temporal repetitive complexity, expecting to overemphasize the differences in the reconstruction between the two groups, dependently on the AA wavefront pattern propagations. This would confirm the parameter suitability in distinguishing between the two AF types. Indeed, $\bar{k}_{0.95}^{AFI}$ is supposed to be suitable for describing around 0.95 of the variance for AF type I recordings, but insufficient for having an acceptable description of AF type III recordings (which are supposed to exhibit higher complexity).

3. Results

3.1. AA spatio-temporal repetitiveness

AA signal reconstruction is generally better for signals classified as AF type I than for signals classified as AF

Table 1. Mean performance parameters for the AA spatio-temporal repetitiveness analysis.

Parameter	AF I	AF III	p -value
$\bar{\rho}$	0.98±0.01	0.92±0.04	$p < 0.01$
NMSE	5.28±1.87	16.44±6.68	$p < 0.01$

Table 2. Mean number of significant components giving a cumulative normalized variance of 0.95 for AA organization analysis.

Parameter	AF I	AF III	p -value
$\bar{k}_{0.95}$	3.64±1.31	8.60±3.80	$p < 0.05$

type III, as underlined by the significant difference in terms of mean ρ reported in Table 1 ($p < 0.01$), which shows also the significant difference in terms of mean NMSEs between the two AF types ($p < 0.01$). Mean parameter values have been calculated averaging over all subjects for the same segment and taking the average over all the segments (for $s = 2, \dots, 6$).

3.2. AA organization

Results on the AA organization analysis are summarized in Table 2. Organization has been assessed in terms of number of principal components $k_{0.95}$ giving a cumulative normalized variance v_k higher than 0.95. Mean values $\bar{k}_{0.95}$ have been obtained averaging $k_{0.95}$ over all segments ($s = 1, \dots, 6$) for the same subject and taking the average over all subjects. Rounded numbers are $\bar{k}_{0.95}^{AFI} = 4$ for AF type I and $\bar{k}_{0.95}^{AFIII} = 9$ for AF type III ($p < 0.05$). This parameter ranged from 1 to 7 for AF type I and from 2 to 17 for AF type III.

3.3. Combined analysis

A fixed number of components $k = 3$ for the reconstruction of any \hat{y}_s was chosen. Three components is close to $\bar{k}_{0.95}^{AFI}$ ($\simeq 4$, Table 2) for AF type I, as confirmed by the mean value of v_k calculated until the third components for AF type I recordings, that is 0.92±0.09, close to 0.95. On the contrary, it is notably different from $\bar{k}_{0.95}^{AFIII}$ ($\simeq 9$), as confirmed by the mean value of v_k calculated until the third component for AF type III, that is 0.78±0.13, considerably smaller than 0.95. Results are summarized in Table 3 (for $s = 2, \dots, 6$).

As expected, significant differences between the two groups have been overemphasized by the combined analysis ($p < 10^{-4}$, for both parameters), and only mean parameter values of AF type III have impaired compared to results presented in Section 3.1, as also showed by the box-and-whiskers plot reported in Fig. 2.

Table 3. Mean performance parameters for the AA spatio-temporal repetitiveness analysis, with $k_{0.95} = 3$.

Parameter	AF I	AF III	p -value
$\bar{\rho}$	0.98 ± 0.01	0.91 ± 0.02	$p < 10^{-4}$
NMSE	4.11 ± 1.57	17.08 ± 3.11	$p < 10^{-4}$

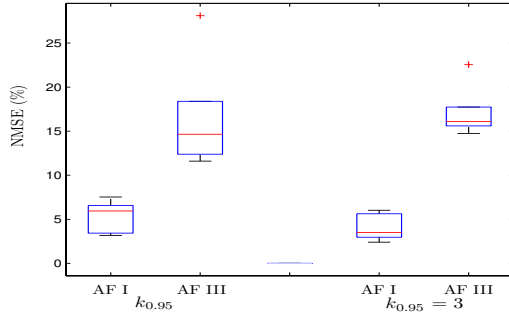


Figure 2. Box-and-whiskers plot for the AA spatio-temporal repetitiveness ($k_{0.95}$) analysis and for the combined one ($k_{0.95} = 3$).

4. Discussion and conclusions

Invasive AF type classifiers are still hardly accepted in clinical practice despite their potential relevance in clinical decision making. Starting from the observations of Guillem *et al.* [4], this work presented a new automated method to assess noninvasively different AF types, based on the high spatial resolution given by BSPM recordings. AF organization degree was assessed through its influence on the spatio-temporal pseudostationarity and complexity of a PCA mixing matrix repeatedly derived along a BSPM recording. The possibility to distinguish among different AF types looking at the AF complexity in terms of number of significant components confirms that the organization of the underlying AA is significantly reflected on the body surface, so that high spatial resolution surface recordings are sufficient to distinguish among different AF types, as claimed in [4]. Moreover, our findings are consistent with those presented by Faes *et al.* [3] obtained studying the extent of repetitiveness in time of the atrial activations within single endocardial recordings. Interestingly, both studies found the same number of significant components necessary to describe 0.95 of the total variance of different types of AF (4 for AF type I, and 9 for AF type III). In conclusion, a greater AF organization has been shown to be reflected in a greater pseudostationarity of the mixing matrix along the recordings and in a lower number of components needed to represent the AA, which can be interpreted as a lower complexity in the underlying AA in patients with organized AF type I, presenting a new way for noninvasive

analysis and diagnosis of AF.

Acknowledgements

The work of P Bonizzi is supported by the EU by a Marie-Curie Fellowship (EST-SIGNAL program: <http://est-signal.i3s.unice.fr>) under contract No MEST-CT-2005-021175. The work of MS Guillem, AM Climent and F Castells was supported by a Spanish Ministry of Science and Innovation under EASI (TEC2008-02193/TEC).

References

- [1] Censi F, Barbaro V, Bartolini P, Calcagnini G, Michelucci A, Gensini GF, et al. Recurrent patterns of atrial depolarization during atrial fibrillation assessed by recurrence plot quantification. *Ann Biomed Eng.* 2000;28:61–70.
- [2] Botteron GW, Smith JM. A technique for measurement of the extent of atrial activation during atrial fibrillation in the intact human heart. *IEEE Trans Biomed Eng.* 1995;42:579–586.
- [3] Faes L, Nollo G, Kirchner M, Olivetti E, Gaita F, Riccardi R, et al. Principal component analysis and cluster analysis for measuring the local organisation of human atrial fibrillation. *Med Biol Eng Comput.* 2001;39:656–663.
- [4] Guillem MS, Climent AM, Castells F, Husser D, Millet J, Arya A, et al. Noninvasive mapping of human atrial fibrillation. *J Cardiovasc Electrophysiol.* 2009;:1–7.
- [5] Konings KT, Kirchhof CJ, Smeets JR, Wellens HJ, Penn OC, Allessie MA. High-density mapping of electrically induced atrial fibrillation in humans. *Circulation.* 1994;89:1665–1680.
- [6] Castells F, Laguna P, Sörnmo L, Bollmann A, Roig JM. Principal component analysis in ECG signal processing. *EURASIP J Appl Signal Process.* 2007;2007(1):98–98.
- [7] Sörnmo L, Laguna P. *Bioelectrical Signal Processing in Cardiac and Neurological Applications.* Amsterdam: Elsevier Academic Press; 2005.
- [8] Rieta JJ, Sánchez C, Sanchis JM, Castells F, Millet J. Mixing matrix pseudostationarity and ECG preprocessing impact on ICA-based atrial fibrillation analysis. *Lecture Notes in Computer Science.* 2004;3195:10791086.

Address for correspondence:

Pietro Bonizzi, Ph.D. Student
 Laboratoire I3S - BIOMED UNSA - CNRS
 2000, Route des Lucioles Les Algorithmes - bât. Euclide B
 B.P. 121, 06903 Sophia Antipolis - Cedex, France
 E-mail: bonizzi@i3s.unice.fr